# Presence of Many Stable Nonhomogeneous States in an Inertial Car-Following Model

Elad Tomer,[1] Leonid Safonov,[1,2] and Shlomo Havlin[1]

[1]*Minerva Center and Department of Physics, Bar–Ilan University, 52900 Ramat-Gan, Israel*
[2]*Department of Applied Mathematics and Mechanics, Voronezh State University, 394693 Voronezh, Russia*
(Received 11 January 1999; revised manuscript received 18 May 1999)

We present a single lane car-following model of traffic flow which is inertial and free of collisions. It demonstrates observed features of traffic flow such as existence of three regimes: free, nonhomogeneous congested (NHC) or synchronized, and homogeneous congested (HC) or jammed flow; bistability of free and NHC flow states in a range of densities, hysteresis in transitions between these states; jumps in the density-flux plane in the NHC regime; gradual spatial transition from synchronized to free flow; long survival time of jams in the HC regime. The model predicts that in the NHC regime there exist many stable states with different wavelengths, and noise can cause transitions between them.

PACS numbers: 45.70.Vn, 89.40.+k

In the last several years, growing effort has been made in understanding traffic flow dynamics. Recent observations [1,2] show that traffic flow demonstrates complex physical phenomena, among which are the following:

(i) The existence of three phases: free flow regime at low densities, NHC (or "synchronized") flow regime at intermediate densities where oscillations of velocities of all cars are observed, and HC or jammed flow regime at high densities. The NHC regime has two essential features: synchronization of flow in different lanes (for the multilane traffic) and fluctuation performed by the system in density-flux plane. Since our model is single lane we will refer to this state as "nonhomogeneous congested."

(ii) Hysteresis in transitions between the free and the NHC flow.

(iii) Long survival time of traffic jams.

Modeling of traffic flow is traditionally performed using two approaches: The microscopic, or car-following model approach, which describes the nearest-neighbor interaction between two consecutive cars and investigates its influence on the flow (see, e.g., [3–6]); and the macroscopic, or continuous model approach, which represents the flowing traffic as a continuous media and describes it using the hydrodynamical partial differential equations (see, e.g., [7–9]). Wide surveys of these models are given in [10–12].

In this Letter, we introduce an inertial single lane car-following model, which (i) demonstrates and explains the experimentally observed phenomena mentioned above, and (ii) shows the existence of many stable NHC states with different wavelengths in the second regime and the possibility of transitions between them in the presence of noise.

To formulate the model we assume that car acceleration is affected by four factors: (a) aspiration to keep safety time gap from the car ahead, (b) prebraking if the car ahead is much slower, (c) aspiration not to exceed significantly the permitted velocity, and (d) random noise. In mathematical description, the acceleration of

the $n$th car $a_n$ is given by a sum of four terms depending on its coordinate $x_n$, velocity $v_n$, distance to the car ahead $\Delta x_n = x_{n+1} - x_n$, and the velocities difference $\Delta v_n = v_{n+1} - v_n$:

$$
a_n = A\left(1 - \frac{\Delta x_n^0}{\Delta x_n}\right) - \frac{Z^2(-\Delta v_n)}{2(\Delta x_n - D)}
$$
$$
- kZ(v_n - v_{\text{per}}) + \eta, \tag{1}
$$

where $A$ is a sensitivity parameter, $D$ is the minimal distance between consecutive cars, $v_{\text{per}}$ is the permitted velocity, $k$ is a constant, and $\eta$ is a white noise term. The safety distance $\Delta x_n^0 = v_n T + D$ depends on $T$, which is the safety time gap constant. The function $Z$ is defined as $Z(x) = (x + |x|)/2$. In further analytical and numerical exploration of the model the noise term $\eta$ is omitted unless otherwise stated.

In the following, we discuss in more detail the terms in the right side of (1):

The first term plays an important role when the velocity difference between consecutive cars is relatively small. In this case the $n$th car accelerates if $\Delta x_n > \Delta x_n^0$ and brakes if $\Delta x_n < \Delta x_n^0$. The choice of function in this term is not unique. Replacing it by other functions of $\Delta x_n$ which are increasing, equal to zero if $\Delta x_n = \Delta x_n^0$ and tend to $-\infty$ if $\Delta x_n \to 0$, such as $A\log(\Delta x_n/\Delta x_n^0)$, gives similar results.

The second term plays an important role when $v_n \gg v_{n+1}$. A car getting close to a much slower car starts braking even if $\Delta x_n > \Delta x_n^0$. This term corresponds to the negative acceleration needed to reduce $|\Delta v_n|$ to 0 as $\Delta x_n \to D$.

The dissipative third term is a repulsive force acting when the velocity exceeds the permitted velocity.

Note that unlike the optimal velocity model [5] the acceleration in our model depends explicitly on $\Delta v_n$ and on $\Delta x_n$ which enables us to make the flow free of collisions.

The motion of cars is therefore described by the following system of ordinary differential equations:

$$\begin{cases} \dot{x}_n = v_n, \\ \dot{v}_n = A\left(1 - \frac{v_n T + D}{x_{n+1} - x_n}\right) \\ \qquad - \frac{Z^2(v_n - v_{n+1})}{2(x_{n+1} - x_n - D)} - kZ(v_n - v_{per}); \end{cases} \quad (2)$$

$n = 1, 2, \ldots, N$ with periodic boundary conditions $x_{N+1} = x_1 + \frac{N}{\rho}$, $v_{N+1} = v_1$.

A solution of Eqs. (2) which corresponds to homogeneous flow is

$$v_n^0 = v^0 = \begin{cases} \frac{A(1 - D\rho) + kv_{per}}{A\rho T + k}, & \rho \leq \frac{1}{D + Tv_{per}}, \\ \frac{1 - D\rho}{\rho T}, & \rho \geq \frac{1}{D + Tv_{per}}, \end{cases} \quad (3)$$

$x_n^0 = \frac{n-1}{\rho} + v^0 t.$

In the following numerical analysis we use parallel updating rule and parameters values $v_{per} = 25(\text{m/s})$, $T = 2(\text{s})$, $D = 5(\text{m})$, $1 \leq A \leq 5(\text{m/s}^2)$, and $k = 2(\text{s}^{-1})$.

The flux-density relation (often called the fundamental diagram) for the homogeneous flow is shown in Fig. 1(a) as a dashed line. Comparison of this curve, with the fundamental diagrams (solid lines) obtained by the numerical solution of Eqs. (2) for different values of $A$ starting from nonhomogeneous initial conditions, indicates that for values of $\rho$ smaller than some critical value $\rho_1$ or greater than another critical value $\rho_2$ the flux is the same, while for the intermediate values of density ($\rho_1 < \rho < \rho_2$) the measured flux is considerably lower than the homogeneous solution flux. Plotting the variance of velocities $\sigma_v = [\frac{1}{N}\sum_{n=1}^{N}(v_n - \langle v \rangle)^2]^{1/2}$ (where $\langle v \rangle$ is the average velocity) against $\rho$ [Fig. 1(b)] shows the existence of velocity fluctuations for $\rho_1 < \rho < \rho_2$. We can therefore define three regimes in traffic flow: the free flow regime ($\rho < \rho_1$), the NHC flow regime ($\rho_1 < \rho < \rho_2$), and the HC flow regime ($\rho > \rho_2$). Note that the flow in the first and the last regimes is homogeneous. Note also that for small values of $A$ $\rho_2$ is greater than the maximal possible density $\rho_{max} = 1/D$ and the HC flow regime does not exist. See Fig. 1(b) for $A = 2$. This finding is supported by the analytical results shown below.

In order to estimate the values of $\rho_1$ and $\rho_2$ we analyze the stability of the homogeneous flow solution. The linearization of Eqs. (2) near the homogeneous flow solution (3) in variables $\xi_n = x_n - x_n^0$ has the form

$$\ddot{\xi}_n = -p\dot{\xi}_n + q(\xi_{n+1} - \xi_n), \quad n = 1, \ldots, N, \quad (4)$$

where $\xi_{N+1} = \xi_1$, $p = AT\rho + k$, $q = \frac{AT + kTv_{per} + kD}{AT\rho + k} \cdot A\rho^2$ for $\rho \leq \frac{1}{D + Tv_{per}}$ and $p = AT\rho$, $q = A\rho$ otherwise.

As in [5] solution of Eq. (4) can be written as

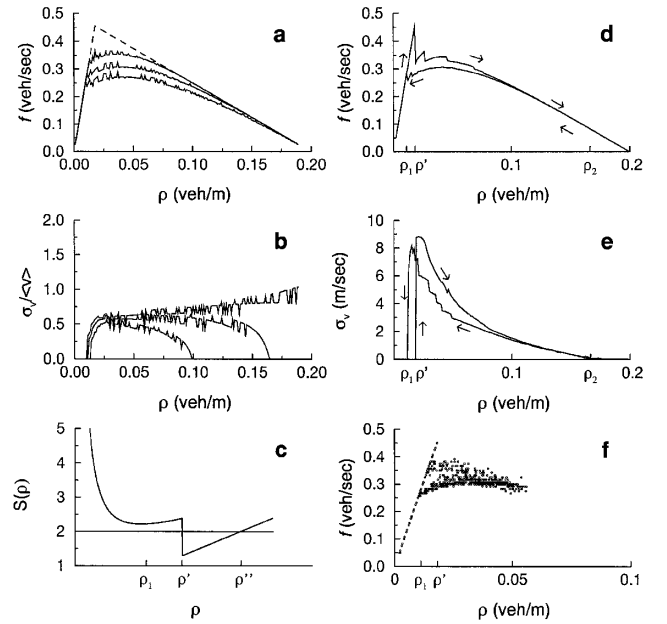$$\xi_n = \exp\{i\alpha n + zt\}, \quad (5)$$



FIG. 1. (a) Fundamental diagram for $A = 5, 3, 2(\text{m/s}^2)$ (top to bottom). Dashed line corresponds to the homogeneous solution. (b) Ratio of variance of velocities to the average velocity for $A = 2, 3, 5(\text{m/s}^2)$ (top to bottom). (c) Qualitative plot of function $S(\rho)$. (d), (e) Hysteresis loops in transitions between free and NHC flow states for $A = 3$; arrows show the direction of changing the global density. (f) Results of local measurements of density and flux in free (almost straight line) and NHC regimes.

where $\alpha = \frac{2\pi}{N}\kappa$ ($\kappa = 0, \ldots, N - 1$) and $z$ is a complex number. Substituting (5) into (4) we obtain the algebraic equation for $z$,

$$z^2 + pz - q(e^{i\alpha} - 1) = 0. \quad (6)$$

Each of the $N$ Eqs. (6) has two solutions. These $2N$ different complex numbers are the eigenvalues of system (4). One of them (which corresponds to $\kappa = 0$) is equal to zero regardless of values of parameters. In this case all $\xi_n$ in (5) are equal to a constant and belong to the one-dimensional subspace of equilibria of system (4) (defined by equations $\xi_1 = \ldots = \xi_N$, $\dot{\xi}_1 = \ldots = \dot{\xi}_N = 0$). This indicates that the disturbed state $x_n$ for $z = 0$ is also homogeneous. For $z \neq 0$, $\xi_n$ in (5) is a wave with increasing or decreasing amplitude. Therefore, if we find conditions under which other $2N - 1$ eigenvalues have negative real parts [the magnitude of wave (5) decreases with time] we can say that under these conditions the homogeneous flow solution (3) is stable.

Following the approach of [5] we can derive this condition as $\frac{p^2}{q} > 2$ or $S(\rho) > 2$, where

$$S(\rho) = \begin{cases} \frac{(AT\rho + k)^3}{\rho^2 A(AT + kv_{per}T + kD)}, & \rho \leq \frac{1}{D + Tv_{per}}, \\ A\rho T^2, & \rho \geq \frac{1}{D + Tv_{per}}. \end{cases} \quad (7)$$

A qualitative plot of $S(\rho)$ is sketched in Fig. 1(c). From this figure it follows that depending on $\rho$ we have three regimes of stability/instability of the homogeneous flow solution. If $\rho < \rho'$ (free flow) or $\rho > \rho''$ (HC flow) the homogeneous flow solution is stable and if $\rho' < \rho < \rho''$ it is unstable, where $\rho' = \frac{1}{D+Tv_{per}}$ and $\rho'' = \frac{2}{AT^2}$. The third regime does not exist for $\rho'' > \rho_{max}$ [e.g., Figs. 1(a) and 1(b) for $A = 2(m/s^2)$]. Our numerical simulations show that $\rho_2 \approx \rho''$, but $\rho'$ is considerably greater than $\rho_1$, thus we expect that for $\rho_1 < \rho < \rho'$ both homogeneous and nonhomogeneous states are stable.

In the NHC regime ($\rho_1 < \rho < \rho_2$) the flow is characterized by the presence of humps (dense regions) moving backwards or forwards. When the flow has stabilized the humps are equidistant and the evolution of traffic in time and space resembles the spreading of a wave. The existence of a NHC regime was predicted by other car-following (e.g., [5] where it was called "jammed flow") and continuous (e.g., [9], where it was called "recurring humps state") models and measured experimentally [1].

Simulations of our model show that the NHC flow state is not unique. Figures 2(a)–2(c) present the car velocities after the NHC flow regime has stabilized for three different initial conditions. It can be seen that the "wavelengths" of these states are different. Figure 2(d) presents the convergence of flux in these experiments to distinct values. Our simulations also show the existence of solutions with other "wavelengths" and flux values. Figure 2(e) shows the fundamental diagrams for three different wavelengths. Consequently, depending on initial conditions, different stable NHC states emerge with different values of flux and distances between neighboring humps. This indicates that for $\rho_1 < \rho < \rho_2$, system (2) has many stable periodic (in $\Delta x_n$, $v_n$ variables) solutions, and hence in the $2N$-dimensional space of variables $\Delta x_n$, $v_n$ there exist many attractive limit cycles.

Our simulations show that some of these cycles are more sensitive to noise than others, and therefore are metastable. For sufficiently large $\eta$ (and below certain threshold) the system moves from these metastable states to those which are stable. It appears that cycles with relatively small and relatively large wavelengths are more sensitive to noise than those with intermediate wavelengths. The space-time diagram in Fig. 3 illustrates this phenomenon. Simulations are started without noise from a homogeneous initial condition with small harmonic disturbance. After the periodic state is stabilized, the noise term ($\eta \neq 0$) is added at $t = 200$ s. The system is then attracted to another stable limit cycle with a *bigger* wavelength. Note that transition from a smaller to a bigger wavelength has been observed recently [13] in real traffic.

As seen from above for $\rho_1 < \rho < \rho'$ not only NHC flow solutions are stable, but also the homogeneous flow solution. This bistability is the origin of hysteresis in transitions between free and NHC flow regimes. Such bistability was observed experimentally [1] and was found in other models [5,6,9]. Figure 1(d) shows a hysteresis loop in the density-flux plane. The upper curve is obtained by increasing the density of cars adiabatically preserving the road length $L$ [14]. It can be seen that up to the value of density $\rho'$ the homogeneous flow is preserved. The lower curve was obtained by adiabatically decreasing the density in the same manner. While decreasing the density, the flow remains nonhomogeneous even for $\rho < \rho'$. Figure 1(e) presents the hysteresis loop in the global density–velocities fluctuations plane.

Our results also illustrate the well-known phenomenon [1,2,5,9,10] of jumps which the system performs in the
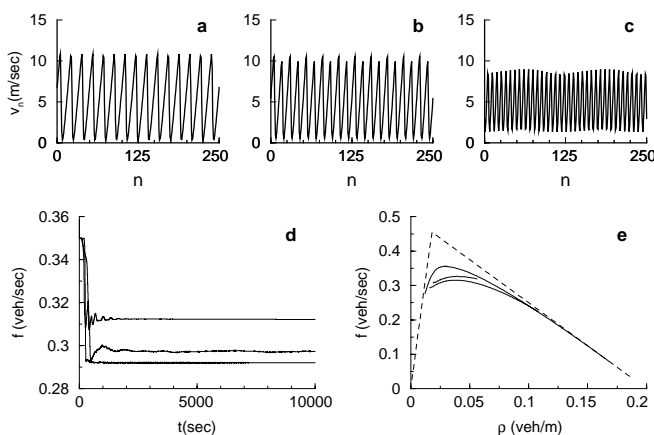
FIG. 2. Three different stable states in the NHC regime, obtained from different initial conditions. Global density $\rho = 0.06$(veh/m), $A = 3$(m/s$^2$). (a)–(c) Car velocities. (d) Convergence of flux to different values in these three experiments. (e) Fundamental diagrams for three different stable NHC states with wavelengths 20, 5, and 6.67 cars (top to bottom). A dashed line corresponds to the homogeneous solution.
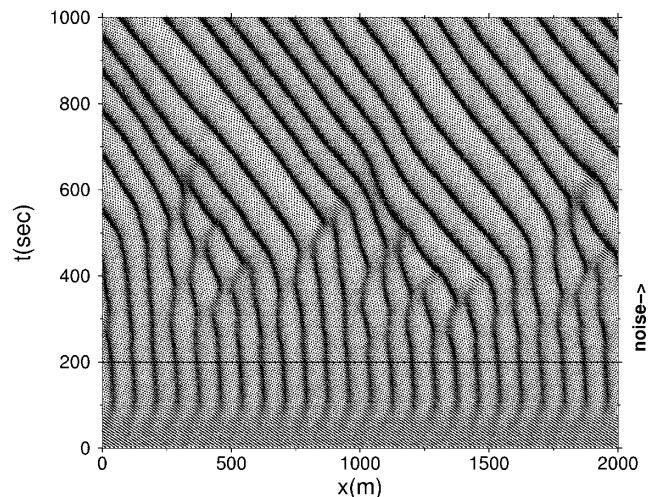
FIG. 3. Transition from a metastable to a stable cycle in presence of noise. $\rho = 0.06$(veh/m), $A = 3$(m/s$^2$), $N = 120$. Noise added at $t = 200$ s.
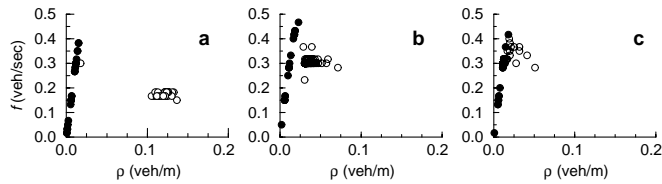
FIG. 4.   Results of local measurements of flux and density at different distances from the on-ramp. (a) 500 m upstream the on-ramp, (b), (c) 250 and 1000 m downstream, respectively. Filled circles—free flow; empty circles—NHC flow.

density-flux plane in the NHC flow regime when the density and the flux are measured locally. In our numerical simulation [Fig. 1(f)] we started from a value of density below $\rho'$, increased it gradually in the described above manner up to a value greater than $\rho'$, and decreased it back. These jumps may be explained by our finding of many stable states in the NHC regime.

Our model also demonstrates the gradual spatial transition from the NHC to free flow in the downstream direction which was measured by [1]. The results of local measurements of density and flux at different distances from an on-ramp [15] are shown in Fig. 4 which is in good agreement with Fig. 3 of [1].

In the HC flow regime the only stable solution is the homogeneous flow solution. We have not found evidence of the existence of bistability or hysteresis in transitions between the NHC and HC flow regimes. Starting from random initial conditions, we observe that initial fluctuations of the velocity seem to decay according to a power law $\sigma_v \sim t^{-\beta}$ for $t \ll t^*$ and exponentially $\sigma_v \sim e^{-t/\tau}$ for $t \gg t^*$. We find $t^* \sim L^z$ and $\tau \sim L^z$ with $z = 2.0 \pm 0.1$. These results are qualitatively similar to that obtained by [16] for a cellular automata model [4], but with different values of exponents. The result $z \approx 2$ seems to be universal for the model and in agreement with random walk arguments of [6]. For the parameters values $A = 4, \rho = 0.15$ we get $\beta \approx 0.21 \pm 0.04$. Relatively slow power-law decay of fluctuations can explain the experimentally observed long survival time of jams [2].

In summary, we present a single lane car-following model which explains important features of traffic observed experimentally. The model predicts the existence of many stable periodic states in the NHC (synchronized) flow regime. We find that some of these states are metastable and have higher sensitivity to noise.

[1] B. S. Kerner and H. Rehborn, Phys. Rev. Lett. **79**, 4030 (1997).
[2] B. S. Kerner and H. Rehborn, Phys. Rev. E **53**, R4275 (1996).
[3] R. Herman and R. W. Rothery, in *Proceedings of the 2nd International Symposium on the Theory of Traffic Flow, London, 1963* (Organization for Cooperation and Development, Paris, 1965).
[4] K. Nagel and M. Schreckenberg, J. Phys. I (France) **2**, 2221 (1992).
[5] M. Bando, K. Hasebe, A. Nakayama, A. Shibata, and Y. Sugiyama, Jpn. J. Ind. Appl. Math. **11**, 203 (1994); Phys. Rev. E **51**, 1035 (1995); M. Bando, K. Hasebe, A. Nakayama, K. Nakanishi, A. Shibata, and Y. Sugiyama, J. Phys. I (France) **5**, 1389 (1995); Y. Sugiyama, in *Proceedings of the Workshop on Traffic and Granular Flow, Julich, 1995,* edited by D. E. Wolf, M. Schreckenberg, and A. Bachem (World Scientific, Singapore, 1996), p. 137.
[6] K. Nagel and M. Paczuski, Phys. Rev. E **51**, 2909 (1995).
[7] B. S. Kerner and P. Konhäuser, Phys. Rev. E **48**, R2335 (1993).
[8] D. Helbing, Phys. Rev. E **51**, 3164 (1995).
[9] H. Y. Lee, H.-W. Lee, and D. Kim, Phys. Rev. Lett. **81**, 1130 (1998).
[10] K. Nagel, Phys. Rev. E **53**, 4655 (1996).
[11] D. E. Wolf, Physica (Amsterdam) **263A**, 438 (1999).
[12] S. Krauss, Ph.D. thesis, Deutsches Zentrum für Luft- und Raumfahrt Hauptabteilung Mobilität und Systemtechnik, Köln, 1998.
[13] B. S. Kerner, Phys. Rev. Lett. **81**, 3797 (1998).
[14] Every new car is placed in the middle between two consecutive cars chosen randomly. The safety time gap is halved and then gradually increased up to the initial value $T$.
[15] Starting from a low value of density (free flow) the density is increased by the influx $f_{in} = 0.133(veh/s)$ at the on-ramp situated at $x_{in} = L/4$, where $L = 100\,00(m)$. The off-ramp is at $x_{out} = 3L/4$ and the outflux changes instantly from 0 to $f_{out} = f_{in}$ when the global density $\rho$ reaches the maximal value $0.03(veh/m)$.
[16] G. Csányi and J. Kertész, J. Phys. A **28**, L427 (1995); M. Sasvári and J. Kertész, Phys. Rev. E **56**, 4104 (1997).